Journal of Power Sources 196 (2011) 764–767

Contents lists available at ScienceDirect

Journal of Power Sources

journal homepage: www.elsevier.com/locate/jpowsour

Short communication

Characterization of the interface between $LiCoO_2$ and $Li_7La_3Zr_2O_{12}$ in an all-solid-state rechargeable lithium battery

Ki Hyun Kim[a,*], Yasutoshi Iriyama[b], Kazuo Yamamoto[a], Shota Kumazaki[b], Toru Asaka[a], Kinuka Tanabe[a], Craig A.J. Fisher[a], Tsukasa Hirayama[a], Ramaswamy Murugan[c], Zempachi Ogumi[d]

[a] Japan Fine Ceramics Center, 2-4-1 Mutsuno, Atsuta-ku, Nagoya 456-8587, Japan
[b] Department of Materials Science and Chemical Engineering, Faculty of Engineering, Shizuoka University, 3-5-1 Johoku, Naka-ku, Hamamatsu, Shizuoka 432-8561, Japan
[c] Department of Physics, Pondicherry Engineering College, Puducherry 605-014, India
[d] Innovative Collaboration Center, Kyoto University, Nishikyo-ku, Kyoto 615-8520, Japan

ARTICLE INFO

Article history:
Received 14 June 2010
Received in revised form 26 July 2010
Accepted 26 July 2010
Available online 1 August 2010

Keywords:
$Li_7La_3Zr_2O_{12}$
Solid electrolyte
Lithium secondary batteries
Electrochemical performance
Interface reaction

ABSTRACT

The interfacial layer formed between a lithium-ion conducting solid electrolyte, $Li_7La_3Zr_2O_{12}$ (LLZ), and $LiCoO_2$ during thin film deposition was characterized using a combination of microscopy and electrochemical measurement techniques. Cyclic voltammetry confirmed that lithium extraction occurs across the interface on the first cycle, although the nonsymmetrical redox peaks indicate poor electrochemical performance. Using analytical transmission electron microscopy, the reaction layer (~50 nm) was analyzed. Energy dispersive X-ray spectroscopy revealed that the concentrations of some of the elements (Co, La, and Zr) varied gradually across the layer. Nano-beam electron diffraction of this layer revealed that the layer contained neither $LiCoO_2$ nor LLZ, but some spots corresponded to the crystal structure of La_2CoO_4. It was also demonstrated that reaction phases due to mutual diffusion are easily formed between LLZ and $LiCoO_2$ at the interface. The reaction layer formed during high temperature processing is likely one of the major reasons for the poor lithium insertion/extraction at LLZ/$LiCoO_2$ interfaces.

1. Introduction

Advanced rechargeable lithium batteries with high energy density are required as power sources for electric or hybrid vehicles. Solid-state batteries (SSBs) with non-flammable inorganic solid electrolytes are one candidate, and various kinds of solid electrolytes consisting of oxide or sulphide compounds have been reported [1–4].

Weppner et al. have recently discovered a series of garnet structured solid electrolytes with high lithium ionic conductivities [5–7]. One of these, lanthanum lithium zirconium oxide ($Li_7La_3Zr_2O_{12}$, LLZ), has received much attention as a next-generation solid electrolyte because of its high lithium ionic conductivity (2×10^{-4} S cm^{-1}) at room temperature and sufficient stability against lithium metal [7]. Although several solid electrolytes, such as lanthanum lithium titanate [1] and sulphide-based glass ceramics [3,4], display higher lithium ionic conductivities, such solid electrolytes are unstable against lithium metal. This stability limitation on the anode side restricts the choice of negative electrode materials to those of higher redox potential, which decreases the possible battery operating voltage. There are other solid electrolytes that have sufficient stability against lithium metal, such as lithium phosphorus oxynitride (LiPON) [8], lithium iodide [9], and lithium nitride [10], but they do not offer high lithium ionic conductivities at room temperature. Their lower lithium ionic conductivity inevitably increases the internal cell resistance, which restricts their application in SSBs almost exclusively to thin-film systems. Therefore, the discovery of LLZ with the above two advantages offers new opportunities for developing large-scale SSBs.

On the other hand, electrode/electrolyte interfacial resistance needs to be reduced to minimize the internal resistance of the battery. Even though the solid electrolyte itself may have sufficient lithium-ion conductivity, the electrode/electrolyte interfacial resistance can be very large, which would retard lithium insertion/extraction across the interface, resulting in a decrease in power density. This problem has been extensively examined in battery systems containing a sulphide-based solid electrolyte with ca. 10^{-3} S cm^{-1} lithium-ion conductivity at room temperature, and a surface coating technique has been reported to be an effective method for reducing the interfacial resistance [11,12]. Ohta et al. have proposed a "space charge model" to explain the reduction of interfacial resistance upon surface coating [11], but the formation of a mutual diffusion layer at the interface is

* Corresponding author at: Nanostructures Research Laboratory, Japan Fine Ceramics Center, 2-4-1 Mutsuno, Atsuta-ku, Nagoya 456-8587, Japan.
Tel.: +81 52 871 3500; fax: +81 52 871 3599.
E-mail address: k_kim@jfcc.or.jp (K.H. Kim).

0378-7753/$ – see front matter © 2010 Elsevier B.V. All rights reserved.
doi:10.1016/j.jpowsour.2010.07.073

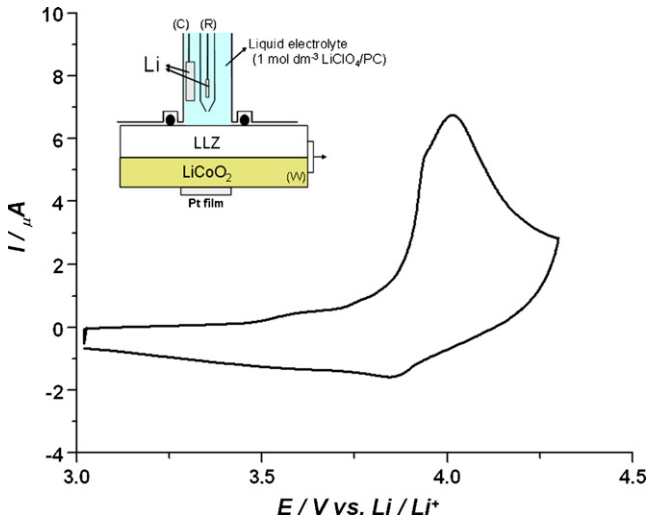

Fig. 1. CVs of the LLZ/$LiCoO_2$ half-cell measured between 3.0 and 4.2 V at room temperature with a scanning rate of 0.1 mV s^{-1}. The electrochemical cell used to measure these CVs is illustrated schematically in the inset.

another possible explanation [12]. Although the role of the surface coating in reducing interfacial resistance is still not clearly understood, these results point to the importance of characterizing the basic interfacial reactions at the electrodes/electrolyte interface that form both during synthesis and during charge/discharge cycles.

In this work, we deposited thin films of $LiCoO_2$ on well-crystallized LLZ pellets, and investigated the interfaces by transmission electron microscopy (TEM). Although there are many kinds of electrode active materials and various combinations with LLZ are possible, we selected $LiCoO_2$ as the electrode material in this work because it is a well-known and typical positive electrode material. Also, it has been shown to work well in various SSB systems [13,14].

2. Experimental

We prepared dense pellets of LLZ (10 mm in diameter, 1–2 mm in thickness) following the procedure reported in Ref. [7]. The pellets were characterized by X-ray diffraction (XRD) using a diffractometer equipped with a CuKα source (Rigaku Ultima IV). The data were collected over a 2θ range of 10–70° at a scan rate of 1° min^{-1}. Platinum thin films were deposited on both sides of the pellets, and lithium-ion conductivities measured by AC impedance spectroscopy.

Thin films of $LiCoO_2$ (approximately 100 nm in thickness) were deposited on one mirror-polished side of each LLZ pellet by pulsed laser deposition at 937 K for 1 h. A lithium-rich sintered Li–Co–O pellet (Li/Co = 1.40) was used as the target, and a fourth-harmonic Nd:YAG laser (266 nm) was focused on the pellet so that the energy

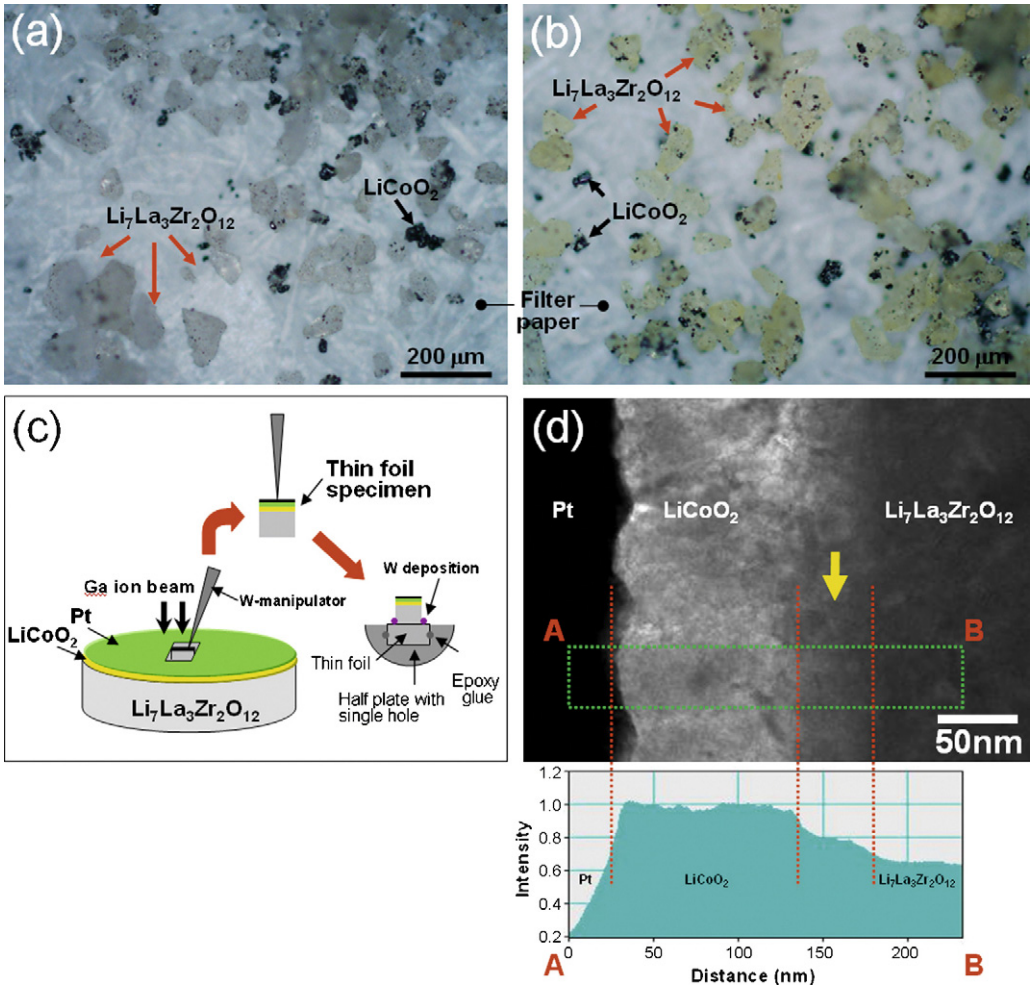

Fig. 2. (a) and (b) Optical micrographs showing the contrast change in $LiCoO_2$/LLZ particles (a) before and (b) after heat-treatment at 973 K; (c) process for preparing a thin foil specimen by FIB micro-sampling; (d) cross-sectional TEM image and intensity profile of the LLZ/$LiCoO_2$ thin film, where the intensity profile was measured in the rectangular region demarcated by broken green lines. The broken red lines indicate the boundaries between the respective layers.

fluence reached 1.0 J cm^{-2} at the target surface. After deposition of the $LiCoO_2$ thin films, the entire surface of each $LiCoO_2$ film was coated with a platinum current collector film by radio frequency magnetron sputtering.

Reactivity between $LiCoO_2$ and LLZ was also investigated using particles of each starting powder. The particles were well mixed in a 1:1 volume ratio using an agate mortar and pestle, and fired at 973 K for 2 h in air. The particles before and after heat-treatment were observed by optical microscopy (Nikon, SM-2800).

Electrochemical properties of the Pt/$LiCoO_2$/LLZ pellets were measured by cyclic voltammetry using a three-electrode cell. A schematic image of the electrochemical measurement cell is given in the inset of Fig. 1. The platinum film side was connected to a stainless steel board. The working electrodes were thin films of $LiCoO_2$. The bare sides of the LLZ pellets were immersed in 1 mol dm^{-3} $LiClO_4$ dissolved in propylene carbonate (PC) solution. Lithium metal immersed in the liquid electrolyte was used as both reference and counter electrodes. Visual inspection did not reveal any leakage of liquid electrolyte through the LLZ pellet. The electrode potential was swept between 3.5 and 4.3 V (vs. Li/Li$^+$) at a potential sweep rate of 0.1 mV s^{-1}.

Analytical TEM measurement was carried out to characterize the LLZ/$LiCoO_2$ interface. A cross-sectional thin sample was prepared with a focused ion beam (FIB) system (Hitachi, FB-2100 with a micro-sampling system) [15]. The thickness of the TEM specimen was approximately 50 nm. Microstructure observation and interface analysis were performed using a 300 kV transmission electron microscope (JEOL, JEM-3000F) equipped with a field emission gun and energy dispersive X-ray spectroscopy (EDS) system (Thermo Noran).

3. Results and discussion

The XRD pattern of the prepared LLZ pellets matched well the standard pattern of the garnet phase $Li_5La_3Nb_2O_{12}$ [16], and diffraction peaks assigned to the pyrochlore phase, $La_2Zr_2O_7$, which is generally formed by the loss of lithium during the preparation process, were not observed at all. Lithium-ion conductivities of the resultant pellets reached approximately 2×10^{-4} S cm^{-1} at room temperature, and the activation energy for lithium-ion conduction was estimated to be 31–34 kJ mol^{-1}. These properties are in good agreement with previous reported values [7].

Fig. 1 shows the cyclic voltammogram (CV) of a Pt/$LiCoO_2$/LLZ pellet measured at 0.1 mV s^{-1} between 3.0 and 4.2 V. The broad oxidation peak at 4.0 V is ascribed to the two-phase reaction of the $LiCoO_2$ thin film electrode. However, a corresponding reduction peak was not clearly discernible. When the film electrodes were deposited on a platinum-coated quartz substrate under the same deposition conditions, the CV measured in 1 mol dm^{-3} $LiClO_4$ dissolved in PC contained reversible two-phase reaction peaks in addition to the order–disorder phase transition reaction peaks of $LiCoO_2$ at 4.1 and 4.2 V, in good agreement with previous results [17]. Therefore, in the CV the broad and asymmetrical two-phase reaction peak, in addition to the indistinct order–disorder phase transition peak, suggests that the LLZ/$LiCoO_2$ interface is detrimental to good battery performance. Furthermore, degradation of the CV was observed even after the second cycle.

The chemical reactivity between $LiCoO_2$ and LLZ was investigated using the starting powder materials. Fig. 2(a) and (b) shows optical micrographs of a mixture of both powders before and after firing at 973 K for 2 h in air. Particles of $LiCoO_2$ were black both before and after firing. In contrast, LLZ particles before firing were gray, with the color changing to green after firing. This distinct color change indicates that a reaction between $LiCoO_2$ and $Li_7La_3Zr_2O_{12}$ occurs at the same temperature at which the thin-film synthesis was carried out.

Analytical TEM was used to investigate the LLZ/$LiCoO_2$ interface in the thin-film sample. The specimen for the TEM measurements was prepared by FIB micro-sampling, as illustrated in Fig. 2(c). First, a rectangular piece of about 20 μm × 5 μm was lifted out of a Pt/$LiCoO_2$/LLZ pellet using a tungsten manipulator in the FIB system. The specimen was then fixed on a TEM grid by tungsten deposition. Finally, it was thinned by FIB to a thickness of approximately 50 nm. A cross-sectional TEM image of the LLZ/$LiCoO_2$ thin film interface is shown in Fig. 2(d). Each layer (the Pt current collector, $LiCoO_2$ thin film, and LLZ) has a different contrast. In the TEM image, an anomalous contrast across a layer approximately 50 nm thick (indicated by a yellow arrow in Fig. 2(d)) can be seen in the vicinity of the LLZ/$LiCoO_2$ interface, almost parallel to each phase. The intensity profile measured along A–B in Fig. 2(d) clearly shows that an anomalous contrast layer exists in the vicinity of the LLZ/$LiCoO_2$ interface.

In general, the change in intensity across each layer is related to the sample's transmissivity, which is a function of the atomic weight of the component atoms in the thin film. A flat profile was observed in both the $LiCoO_2$ and LLZ regions, indicating that each material has an essentially homogeneous composition. However, the intensity gradually decreased in the anomalous contrast region, indicating a heterogeneous distribution of atoms in this region.

To evaluate the anomalous contrast layer quantitatively, we performed EDS analysis across the LLZ/$LiCoO_2$ interface. Fig. 3(a) shows a cross-sectional TEM image across which an EDS line profile was measured from left to right in the region indicated by red solid lines across the LLZ/$LiCoO_2$ interface. The probe diameter for EDS analysis was approximately 5 nm. The EDS line profile (Fig. 3(b))

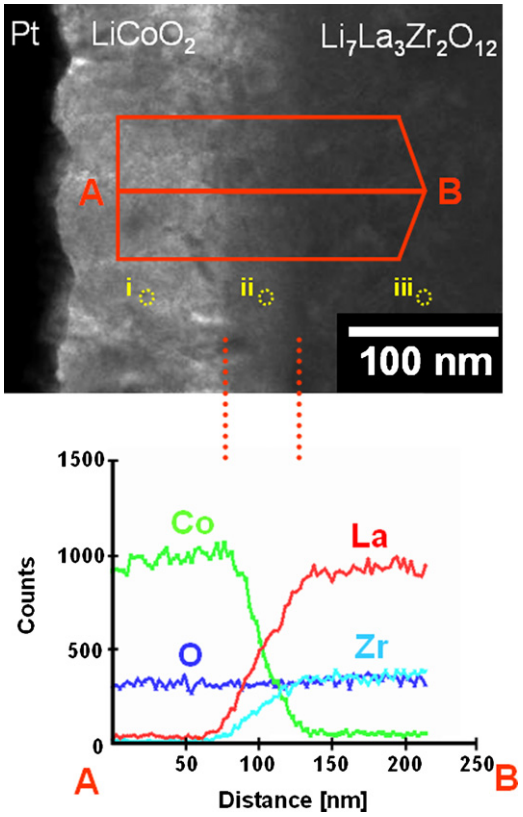

Fig. 3. (a) Cross-sectional TEM image of an LLZ/$LiCoO_2$ thin film interface and (b) the EDS line profile obtained from the region indicated by the red arrow in the direction A–B. The broken red lines indicate the reaction layer at the LLZ/$LiCoO_2$ interface. Points i, ii and iii indicate locations used for NBD analysis. (For interpretation of the references to color in this figure legend, the reader is referred to the web version of the article.)

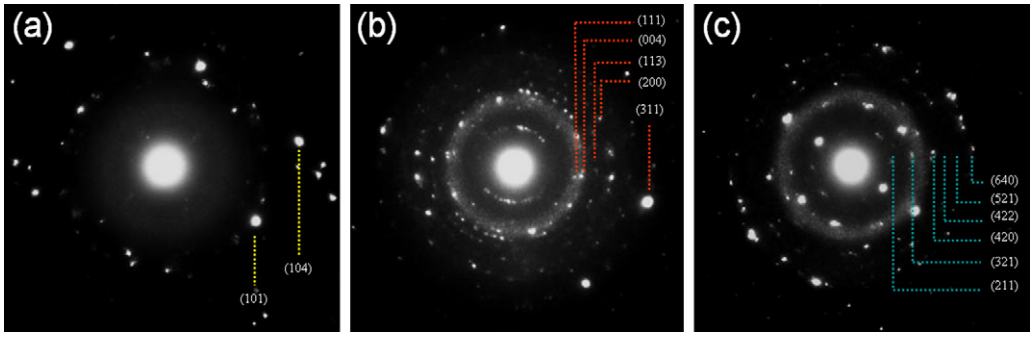

Fig. 4. NBD patterns observed in the (a) $LiCoO_2$ thin film, (b) reaction layer, and (c) LLZ, for regions indicated by broken yellow circles i, ii and iii, respectively, in Fig. 3(a). (For interpretation of the references to color in this figure legend, the reader is referred to the web version of the article.)

revealed that the concentration of Co, La, and Zr varies gradually across this intermediate layer (the region demarcated by red dotted lines in Fig. 3(a)). Because elements from both $LiCoO_2$ and LLZ are found in this region, this intermediate layer is most likely formed as a reaction phase by mutual diffusion of elements between LLZ and $LiCoO_2$ during deposition of the thin film electrodes at 973 K. This conclusion is supported by surface reaction layer observed by optical microscopy of powder particles after heating.

To investigate the reaction phases, nano-beam electron diffraction (NBD) was performed using an electron beam probe diameter of approximately 1–2 nm. Fig. 4(a)–(c) shows the NBD patterns measured at points marked by yellow circles "i", "ii" and "iii", respectively, in Fig. 3(a). The NBD patterns measured in the $LiCoO_2$ thin film (Fig. 4(a)) and LLZ (Fig. 4(c)) are in good agreement with the crystal structures determined by XRD. On the other hand, the NBD pattern obtained from the anomalous contrast layer (Fig. 4(b)) includes diffraction spots that cannot be assigned to either $LiCoO_2$ or LLZ; instead they correspond to La_2CoO_4. Although no other reaction phase was clearly discernible, the concentration gradients of Co, La and Zr shown in Fig. 3 suggest the formation of such reaction phases. When the $LiCoO_2$ thin film was removed from LLZ by polishing, the LLZ surface was green in appearance, which was identical to that observed after heating of particles (Fig. 2(a) and (b)). Since LLZ in contact with both thin films and powders of $LiCoO_2$ at 973 K showed the same color change, it can be concluded that the chemical reaction between $LiCoO_2$ and LLZ occurs during the thin film deposition process; it is a fundamental chemical reaction to form a more thermodynamically stable phase.

In the case of the lanthanum lithium titanate (LLT)/$LiCoO_2$ heterointerface, it has been reported that micro-crack formation at the interface during electrochemical measurement might be the cause of the asymmetrical CV [18]. However, for that system, no reaction phase was observed at the interface, unlike for LLZ/$LiCoO_2$. Formation of a reaction phase by mutual diffusion is generally recognized as improving the adhesion between the two components, so less micro-cracking can be expected at LLZ/$LiCoO_2$ interfaces, and thus less of a contribution from micro-cracking to the interfacial resistance. However, the CV in Fig. 1 is much worse than that of a typical LLT/$LiCoO_2$ system, especially for the lithium insertion process. The similarity between the oxidation peak in Fig. 1 and that measured for a system made from MgO modified $LiCoO_2$ [17] suggests that the reaction phase also forms upon charge/discharge cycling. We thus speculate that the reaction phase in the LLZ/$LiCoO_2$ system increases in size or otherwise undergoes further changes during electrochemical measurements. This complex phenomenon is the subject of ongoing investigations which will be reported in a forthcoming paper.

The above results show that reactive layer formation during processing severely limits the performance capability of SSBs that use LLZ solid electrolytes. As with the sulphide-based solid electrolyte system [12], surface coating or interfacial modification to avoid such a reaction phase may be an effective method to improve the electrochemical properties of such SSBs.

4. Conclusions

We prepared thin films of $LiCoO_2$ on $Li_7La_3Zr_2O_{12}$ (LLZ) pellets and characterized the interface between them by both electrochemical measurement and analytical transmission electron microscopy. Lithium insertion/extraction at the interface was confirmed by CV, but the electrochemical performance was poor. Transmission electron microscopy revealed that an intermediate reaction layer with a thickness of approximately 50 nm forms in the vicinity of the LLZ/$LiCoO_2$ interface during synthesis. From the EDS line profile and nano-beam diffraction taken in the vicinity of the interface, the reaction layer was found to consist of La_2CoO_4. The poor lithium insertion/extraction behavior can be ascribed to the formation of this relatively thick reaction phase at the LLZ/$LiCoO_2$ interface. Suppressing the formation of such a reaction phase will be necessary and effective for developing advanced all-solid-state rechargeable lithium batteries with LLZ as the solid electrolyte.

Acknowledgement

This work was financially supported by the RISING project of the New Energy and Industrial Technology Development Organization (NEDO).

References

[1] Y. Inaguma, L.Q. Chen, M. Itoh, T. Nakamura, T. Uchida, H. Ikuta, M. Wakihara, Solid State Commun. 86 (1993) 689.
[2] J. Fu, J. Am. Ceram. Soc. 80 (1997) 1901.
[3] R. Kanno, M. Maruyama, J. Electrochem. Soc. 148 (2001) A742.
[4] A. Hayashi, S. Hama, T. Minami, M. Tatsumisago, Electrochem. Commun. 5 (2003) 111.
[5] V. Thangadurai, W. Weppner, J. Solid State Chem. 179 (2006) 974.
[6] R. Murugan, V. Thangadurai, W. Weppner, Ionics 13 (2007) 195.
[7] R. Murugan, V. Thangadurai, W. Weppner, Angew. Chem. Int. Ed. 46 (2007) 7778.
[8] J.B. Bates, N.J. Dudney, G.R. Gruzalski, R.A. Zuhr, A. Choudhury, C.F. Luck, J.D. Robertson, Solid State Ionics 53–56 (1992) 647.
[9] D.C. Ginnings, T.E. Phipps, J. Am. Chem. Soc. 52 (1930) 1340.
[10] U.V. Alpen, G. Muller, J. Electrochem. Soc. 124 (1977) C271.
[11] N. Ohta, K. Takada, L.Q. Zhang, R.Z. Ma, M. Osada, T. Sasaki, Adv. Mater. 18 (2006) 2226.
[12] A. Sakuda, A. Hayashi, M. Tatsumisago, Chem. Mater. 22 (2010) 949.
[13] J.B. Bates, N.J. Dudney, B. Neudecker, A. Ueda, C.D. Evans, Solid State Ionics 135 (2000) 33.
[14] Y. Iriyama, T. Kako, C. Yada, T. Abe, Z. Ogumi, Solid State Ionics 176 (2001) 2371.
[15] H. Sasaki, T. Matsuda, T. Kato, T. Muroga, Y. Iijima, T. Saitoh, F. Iwase, Y. Yamada, T. Izumi, Y. Shiohara, T. Hirayama, J. Electron Microsc. 53 (2004) 497.
[16] H. Hyooma, K. Hayashi, Mater. Res. Bull. 23 (1988) 1399.
[17] Y. Iriyama, H. Kurita, I. Yamada, T. Abe, Z. Ogumi, J. Power Sources 137 (2004) 111.
[18] K. Kishida, N. Wada, Y. Yamaguchi, K. Tanaka, Y. Iriyama, Z. Ogumi, H. Inui, Mater. Res. Soc. Symp. Proc. 972 (2007) 251.